

PNNL-32040

Tritium Diffusion in Fe-Al Aluminide Coating Bulk Phases

September 2021

Michel Sassi
David J. Senor

DISCLAIMER

This report was prepared as an account of work sponsored by an agency of the United States Government. Neither the United States Government nor any agency thereof, nor Battelle Memorial Institute, nor any of their employees, **makes any warranty, express or implied, or assumes any legal liability or responsibility for the accuracy, completeness, or usefulness of any information, apparatus, product, or process disclosed, or represents that its use would not infringe privately owned rights.** Reference herein to any specific commercial product, process, or service by trade name, trademark, manufacturer, or otherwise does not necessarily constitute or imply its endorsement, recommendation, or favoring by the United States Government or any agency thereof, or Battelle Memorial Institute. The views and opinions of authors expressed herein do not necessarily state or reflect those of the United States Government or any agency thereof.

PACIFIC NORTHWEST NATIONAL LABORATORY
operated by
BATTELLE
for the
UNITED STATES DEPARTMENT OF ENERGY
under Contract DE-AC05-76RL01830

Printed in the United States of America

Available to DOE and DOE contractors from
the Office of Scientific and Technical
Information,
P.O. Box 62, Oak Ridge, TN 37831-0062
www.osti.gov
ph: (865) 576-8401
fox: (865) 576-5728
email: reports@osti.gov

Available to the public from the National Technical Information Service
5301 Shawnee Rd., Alexandria, VA 22312
ph: (800) 553-NTIS (6847)
or (703) 605-6000
email: info@ntis.gov
Online ordering: <http://www.ntis.gov>

Tritium Diffusion in Fe-Al Aluminide Coating Bulk Phases

September 2021

Michel Sassi
David J. Senior

Prepared for
the U.S. Department of Energy
under Contract DE-AC05-76RL01830

Pacific Northwest National Laboratory
Richland, Washington 99354

Summary

Density functional theory simulations have been carried out to investigate the diffusion of interstitial tritium (T, ^3H) in three Al-rich (>60% at. Al) iron aluminide phases which were observed by STEM imaging in the Fe-Al coating of archive material for Cycle 13. The phases identified were hexagonal FeNiAl₅, monoclinic Fe₄Al₁₃, and orthorhombic Fe₂Al₅. An analysis of the structures of FeNiAl₅ and Fe₄Al₁₃ indicates that these phases can be viewed as the stacking of two layers. The structural particularity of Fe₂Al₅, is that channels are present along the *c*-axis. These channels have a variable Al vacancy content, giving rise to an approximate composition of Fe₂Al₅. Therefore, three stoichiometries for Fe₂Al_{*x*} phase, namely Fe₂Al₄, Fe₂Al₅, and Fe₂Al₆, have been studied to evaluate the impact of Al vacancy concentration on tritium diffusion behavior.

Simulations using the nudged elastic band method indicated that tritium has preferential diffusion pathways in FeNiAl₅ and Fe₄Al₁₃. In FeNiAl₅, tritium preferentially diffuses along the *a*-axis in between layers, while in Fe₄Al₁₃, tritium preferentially diffuses across layers, along the *b*-axis. The energy barriers calculated for these pathways are 0.78 eV and 0.56 eV for FeNiAl₅ and Fe₄Al₁₃ respectively. In the case of Fe₂Al_{*x*} phases, it was found that the tritium diffusion pathway is affected by the Al vacancy concentrations in the channels. In Fe₂Al₄ (i.e., 100% Al vacancy), tritium essentially diffuses at the center of the channel with a small energy barrier of 0.04 eV. In Fe₂Al₅ (i.e., 50% Al vacancy), the diffusion pathway is more complex as the position of tritium oscillates between the center of the channel and the channel's wall, and involves an energy barrier of 1.34 eV. It is worth noting that the lowest energy position of tritium in Fe₂Al₅ is in between two Al atoms, at the center of the channel. In Fe₂Al₆ (i.e., 0% Al vacancy) tritium essentially diffuses along the channel's wall with an energy barrier of 0.18 eV.

The diffusion coefficients, D_T , of tritium in each Fe-Al phase have been estimated using the Einstein-Smoluchowski relation. For FeNiAl₅ and Fe₄Al₁₃, the coefficients are $1.04 \times 10^{-13} \text{ m}^2 \cdot \text{s}^{-1}$ and $2.07 \times 10^{-12} \text{ m}^2 \cdot \text{s}^{-1}$ respectively at 600 K. In the case of Fe₂Al_{*x*} phases, a large disparity is obtained as the coefficients calculated are $2.14 \times 10^{-7} \text{ m}^2 \cdot \text{s}^{-1}$, $2.70 \times 10^{-18} \text{ m}^2 \cdot \text{s}^{-1}$, and $1.27 \times 10^{-8} \text{ m}^2 \cdot \text{s}^{-1}$ at 600 K for Fe₂Al₄, Fe₂Al₅, and Fe₂Al₆ respectively. Among these coefficients, the value calculated for Fe₂Al₅ is surprisingly low (by ~10 orders of magnitude) compared to that of Fe₂Al₄, and Fe₂Al₆. This could be an artifact of the simulations, in which the atomistic model used to calculate the energy barriers in Fe₂Al₅ requires to have fixed Al positions in the channels. In reality, those channels are fast diffusion pathways for Al, which implies that the position of Al atoms is dynamic. As the lowest energy position of tritium in Fe₂Al₅ is in between two Al atoms, at the center of the channel, we suspect that the diffusion of tritium is limited by the diffusion rate of Al in the channels. Sakidja *et al.* have calculated the energy barrier for Al diffusion in the channels (0.52 eV) and by using the Einstein-Smoluchowski relation, we found $D_{\text{Al}} \approx 10^{-11} \text{ m}^2 \cdot \text{s}^{-1}$ at 600 K. Therefore, in the Fe₂Al_{*x*} phases, the tritium diffusion coefficient is likely ranging from 10^{-7} to $10^{-11} \text{ m}^2 \cdot \text{s}^{-1}$ depending on the Al vacancy concentration in the channels.

Altogether, we found that at 600 K tritium diffuses faster in the channels of Fe₂Al_{*x*} phases ($D_T \leq 10^{-11} \text{ m}^2 \cdot \text{s}^{-1}$), then in Fe₄Al₁₃ ($D_T \approx 10^{-12} \text{ m}^2 \cdot \text{s}^{-1}$), and finally in FeNiAl₅ ($D_T \approx 10^{-13} \text{ m}^2 \cdot \text{s}^{-1}$). We also find that interstitial tritium generally diffuses faster in Fe-Al coating phases than in $\gamma\text{-LiAlO}_2$ pellet ($D_T \approx 10^{-14} \text{ m}^2 \cdot \text{s}^{-1}$).

1.0 Introduction

In the design of the TPBAR,¹ an aluminide coating essentially made of Fe-Al phases is in contact with an inner helium filled gas plenum, separating the getter and the 316 stainless steel cladding. While the primary purpose of the getter is to absorb the molecular tritium generated in γ -LiAlO₂ pellets during neutron irradiation, reports^{2,3} have indicated that a small but steady fraction of tritium permeates out of the TPBAR during production. While attempts to mitigate tritium release in the coolant by modifying the design of the TPBAR were ineffective,² it has been recognized that efforts should be devoted to developing an understanding of the irradiation behavior of the various TPBAR components and a mechanistic understanding of tritium transport within the TPBAR during irradiation.

In order to address knowledge gaps related to microstructure evolution in neutron irradiated TPBAR components, Edwards *et al.*⁴ used scanning transmission electron microscopy (STEM) to characterize the structure of Fe-Al coating from archive material for Cycle 13. Among the key results obtained, images analysis and chemical mapping revealed the presence of three Al-rich (>60% at. Al) iron aluminide phases in unirradiated coating. As shown in Figure 1, these phases were identified as hexagonal FeNiAl₅, monoclinic Fe₄Al₁₃, and orthorhombic Fe₂Al₅.

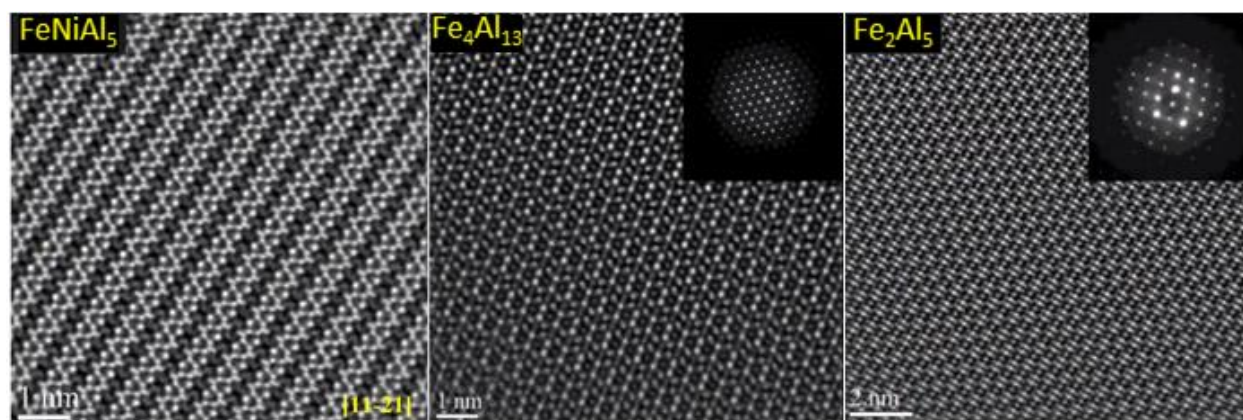


Figure 1: STEM images of Fe-Al bulk phases from the archive coating material for Cycle 13. Courtesy of D. Edwards.⁴

Because Al-rich iron aluminides are known to be brittle,^{5,6} and are difficult to manufacture in bulk, experimental data is sparse, especially regarding hydrogen or tritium diffusion. However, in the case of Fe₂Al₅, previous *ab initio* modellings^{7,8} have indicated that a slight excess of Al (e.g., Fe₂Al_{5.6}) would further stabilize the bulk structure of this phase, which is an approximate composition,⁹ and that at high temperature (1300 K) Al atoms are diffusing in a liquid-like manner along the *c*-axis due to the presence of Al vacancies (V_{Al}) in the structure.

In order to develop a mechanistic understanding of tritium transport in the Al-rich iron aluminide coating phases, we have performed density functional theory simulations in combination with nudged elastic band calculations to estimate the energy barriers for interstitial tritium diffusion. Subsequently, we used the Einstein-Smoluchowski relation to estimate the diffusion coefficients of interstitial tritium in each Fe-Al phases.

2.0 Computational Details

First-principles simulations based on density functional theory (DFT) were carried out using the VASP package.¹⁰ All the simulations used the generalized gradient approximation (GGA) exchange-correlation as parametrized in the Perdew, Burke, and Ernzerhof (PBE) functional.¹¹ A cutoff energy of 350 eV for the plane-wave basis set has been used and spin-polarization has been taken into account. Prior to introducing interstitial tritium, the lattice parameters and atomic coordinates of defect-free supercells of FeNiAl₅,¹² Fe₄Al₁₃,¹³ and three Fe₂A_x phases,^{8,9} namely Fe₂Al₄, Fe₂Al₅, and Fe₂Al₆, were fully relaxed using a convergence criterion of 10⁻⁵ eV/cell for the total energy and 10⁻⁴ eV/Å for the force components. Table 1 summarizes the supercell sizes and Monkhorst-Pack¹⁴ *k*-point mesh used to sample the Brillouin zone in each case. After the addition of interstitial tritium, only the atomic coordinates were allowed to relax, while the lattice parameters were kept fixed to their relaxed defect-free bulk structures values. Due to their similar electronic structure, the pseudopotential of standard hydrogen (¹H) has been used to describe tritium (³H), however, to account for the isotopic effect, the mass in the pseudopotential has been modified to matches that of the isotope atom. For each structure, several diffusion pathways have been investigated and the energy barrier has been determined by using the climbing image nudged elastic band method^{15,16} (CI-NEB). In this study, we focused on neutral interstitial tritium atoms.

Fe-Al phase	Supercell size	<i>k</i> -point mesh
FeNiAl ₅	2×2×2 (224 atoms)	2×2×2
Fe ₄ Al ₁₃	1×1×1 (102 atoms)	2×4×3
Fe ₂ Al ₄	2×2×3 (144 atoms)	2×2×2
Fe ₂ Al ₅	2×2×3 (168 atoms)	2×2×2
Fe ₂ Al ₆	2×2×3 (192 atoms)	2×2×2

Table 1: Summary of the supercell sizes and Monkhorst-Pack *k*-point mesh sampling used in this study.

3.0 Results and Discussion

3.1 Tritium diffusion in FeNiAl₅

Structure of FeNiAl₅. The model structure of hexagonal FeNiAl₅ (space group $P6_3/mmc$, #194) initially used the experimental data from Eliner *et al.*¹² In order to find the most energetically favorable relative positions of Fe and Ni, we simulated six different configurations. The relaxed lattice parameters of the lowest energy structure, shown in Figure 2, are $a=b=7.712$ Å (+0.12%), $c=7.618$ Å (-0.65%), and $\gamma=120^\circ$, which is in good agreement with experimental values ($a=b=7.703$ Å, $c=7.668$ Å, and $\gamma=120^\circ$). An analysis of the structure shows that FeNiAl₅ is made of the stacking of two layers, labelled layer #1 and layer #2, in Figure 2, rotated by 60° . These layers have complementary Fe/Ni content such that layer #1 is made of 25% Fe and 75% Ni and layer #2 is made of 75% Fe and 25% Ni. Interestingly, both layers present some empty spaces which potential for interstitial tritium diffusion across layer will be explored. Because of these empty spaces, columns of Fe or Ni are obtained along the c -axis in which either Fe or Ni atoms populate the column every other layer.

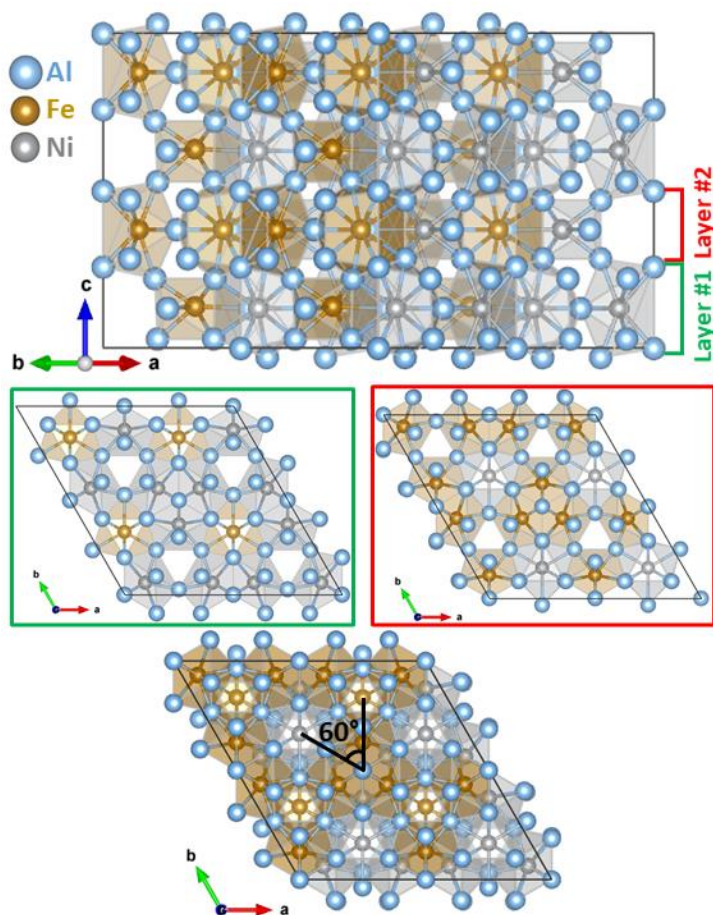


Figure 2: Representation of the bulk structure of hexagonal FeNiAl₅.

Diffusion pathways in FeNiAl₅. As FeNiAl₅ has a high symmetry structure, only two diffusion pathways have been investigated. The energy diagram and visual representation of the diffusion pathway of tritium along the *a*-axis is shown in Figure 3a. To facilitate the visual association between energy and position of tritium along the pathway, we have color-coded both, the dots in the energy diagram and the positions occupied by tritium along the pathway. In this color-code, the lowest energy positions have black color, local minima have blue color, transition states or high energy positions have red color, and the energy and positions which are the transitions between low and high energy positions have green color. Figure 3a shows that the diffusion of interstitial tritium along the *a*-axis requires to overcome an energy barrier of 0.78 eV. Along this pathway, the lowest energy minimum is obtained when tritium is in contact with Fe and forms a Fe—T bond of 1.539 Å. The tritium positions corresponding to a local minimum, of energy 0.40-0.44 eV higher than the lowest energy positions, are related to Ni—T bonds. At image #7, the Ni—T bond length is 1.632 Å, which is about 0.1 Å larger than the Fe—T bonds at images #0 and #14.

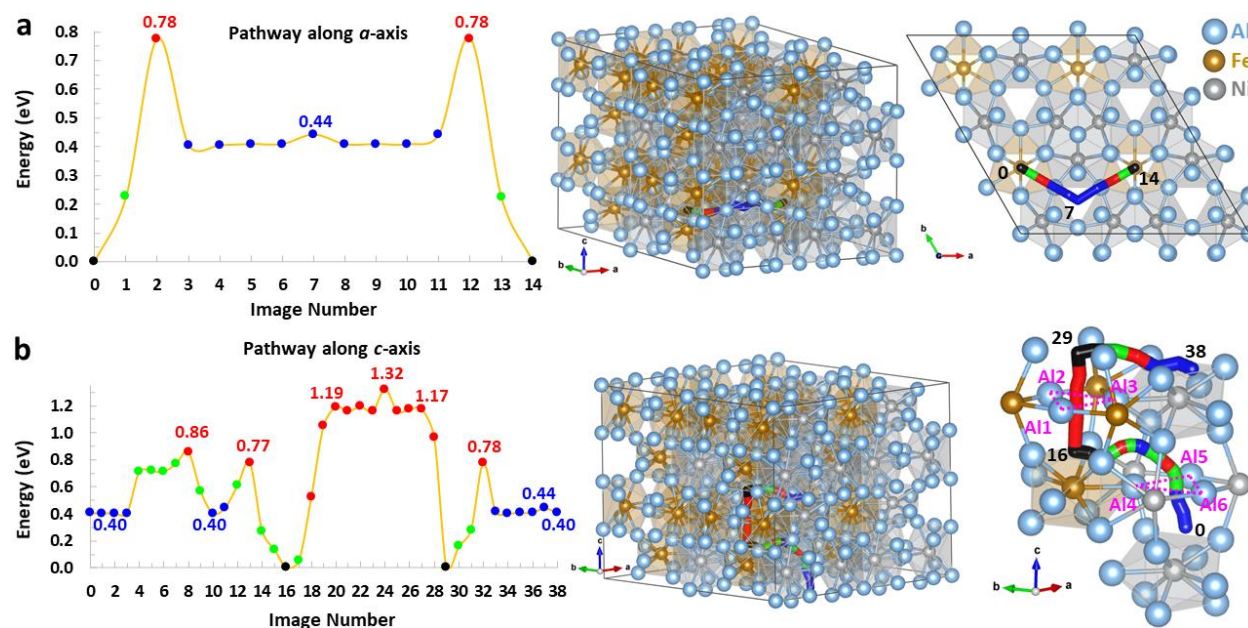


Figure 3: Energy diagrams and representation of the diffusion pathways for tritium in FeNiAl₅. (a) Diffusion pathway parallel to the layers, along the *a*-axis. (b) Diffusion pathway across layers, along the *c*-axis. In the visual representations, some atoms have been removed for clarity. See main text for color-coding.

The diffusion pathway of tritium along the *c*-axis is shown in Figure 3b. In this pathway a series of high energy positions for tritium are obtained from images #19 to #27. These positions correspond to tritium passing at the center of a triangle made with Fe atoms at the corner and Al atoms on the edges. A large energy barrier of 1.19 eV (image #19) is required to pass through this triangle for which an energetically favorable Fe—T bond (image #16) need to be broken. The distances between the Al atoms, labelled AI1, AI2, and AI3 in Figure 3b, are AI1—AI2=AI2—AI3=3.010 Å and AI3—AI1=3.078 Å. In comparison, tritium passing at the center of a triangle made of Ni atoms at the corner and Al atoms on the edges involves a lower energy barrier of 0.46 eV, as obtained between image #3 and image #8. In such triangle, the distances between AI4, AI5, and AI6, as shown in Figure 3b, are AI4—AI5=3.174 Å and AI5—AI6=AI6—AI4=3.180 Å.

Interestingly, the area available for tritium diffusion in the Fe and Ni triangles is 3.98 \AA^2 and 4.37 \AA^2 respectively, which yields to 9.80% more area for the Ni triangle than for the Fe triangle.

These results suggest that interstitial tritium would preferentially diffuse along the a -axis, in between two layers, rather than along the c -axis, across two layers. However, a hybrid pathway between these two cases can also be possible. Such pathway would involve a diffusion of tritium from the image #0 to #7 along the a -axis (Figure 3a), then from image #0 to #16 along the c -axis (Figure 3b). In this hybrid case, the energy barrier of 0.34 eV (difference between image #7 and #12 in Figure 3a) is replaced by a barrier of 0.46 eV (difference between image #0 and #8 in Figure 3b). This hybrid pathway takes advantage of the weaker Ni—T bond compared to Fe—T and the smaller energy barrier required to pass through the Ni triangle with the Al4, Al5, Al6 atoms.

3.2 Tritium diffusion in $\text{Fe}_4\text{Al}_{13}$

Structure of Fe_4Al_5 . The model structure of monoclinic $\text{Fe}_4\text{Al}_{13}$ (space group $C2/m$, #12), shown in Figure 4, used the experimental data from Grin *et al.*¹³ The relaxed lattice parameters are $a=15.423 \text{ \AA}$ (-0.45%), $b=8.025 \text{ \AA}$ (-0.66%), $c=12.422 \text{ \AA}$ (-0.39%), and $\beta=107.70^\circ$ (+0.01%), which is in good agreement with the experimental values of $a=15.492 \text{ \AA}$, $b=8.078 \text{ \AA}$, $c=12.471 \text{ \AA}$, and $\beta=107.69^\circ$. Similarly to FeNiAl_5 , the structure of $\text{Fe}_4\text{Al}_{13}$ is a stacking of two layers, labeled layer #1 and layer #2 in Figure 4, which are shifted by $\frac{1}{2}$ along the a -axis. Interestingly, each layer contains two star-shaped empty spaces connected by an Al corner atom.

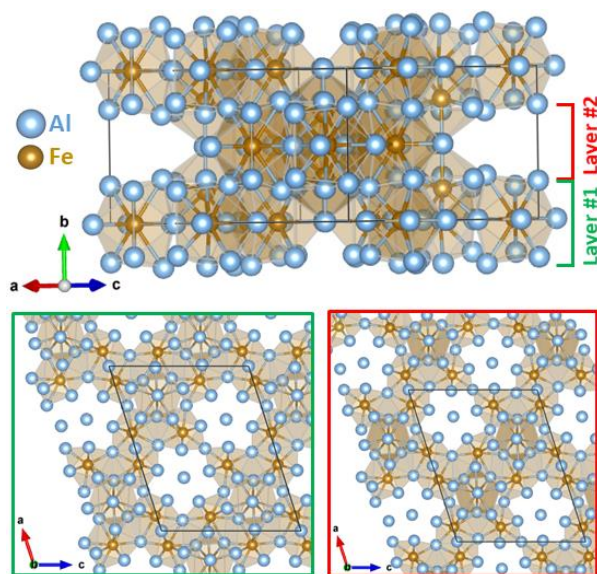


Figure 4: Representation of the bulk structure of monoclinic $\text{Fe}_4\text{Al}_{13}$.

Diffusion pathways in Fe_4Al_5 . Due to the low symmetry of the structure, four diffusion pathways have been investigated for interstitial tritium diffusion in $\text{Fe}_4\text{Al}_{13}$. A diffusion in the (a,c) plane between two star-shaped empty spaces has been studied and is shown in Figure 5a. The largest energy barrier involved in this pathway is 0.98 eV which is obtained for tritium positions between image #3 and #1. Along this pathway, tritium has two lowest energy positions (images #3 and #8) in which it is located at the center of Al triangles, as highlighted by the magenta dashed lines in

Figure 5a. At those positions, the shortest Al—T bond length is about 1.686 Å. A local minimum position is found at images #5 and #6 when tritium cross over the Al atom connecting two star-shaped spaces. At those positions, the local minimum is about 0.52 eV less favorable than the lowest energy positions.

In addition to the diffusion pathway in the (a,c) plane, we investigated three diffusion pathways along the *b*-axis, labeled b1, b2, and b3, and shown in Figure 5b,5c, and 5d respectively. In those diffusion pathways, tritium migrates perpendicularly across the layers. The largest energy barrier calculated is 0.56 eV, 0.84 eV, and 0.83 eV along the pathway b1, b2, and b3 respectively. As all the pathways along the *b*-axis involve lower energy barriers than that in the (a,c) plane, a migration of tritium across layer would be more favorable. Focusing on the pathway b1, which involves the lowest energy barrier of the four pathways investigated, we find a local minimum of 0.49 eV periodically repeating every 4.978 Å at images #0, #8, and #16. At this local minimum, tritium passes in between two Al atoms, with the shortest Al—T distance being 1.809 Å. At the lowest energy positions (images #4 and #12), periodically repeating every 4.974 Å, tritium is located at the center of a Al square, as highlighted by magenta balls in Figure 5b. At these locations, the shortest Al—T contact is 1.849 Å.

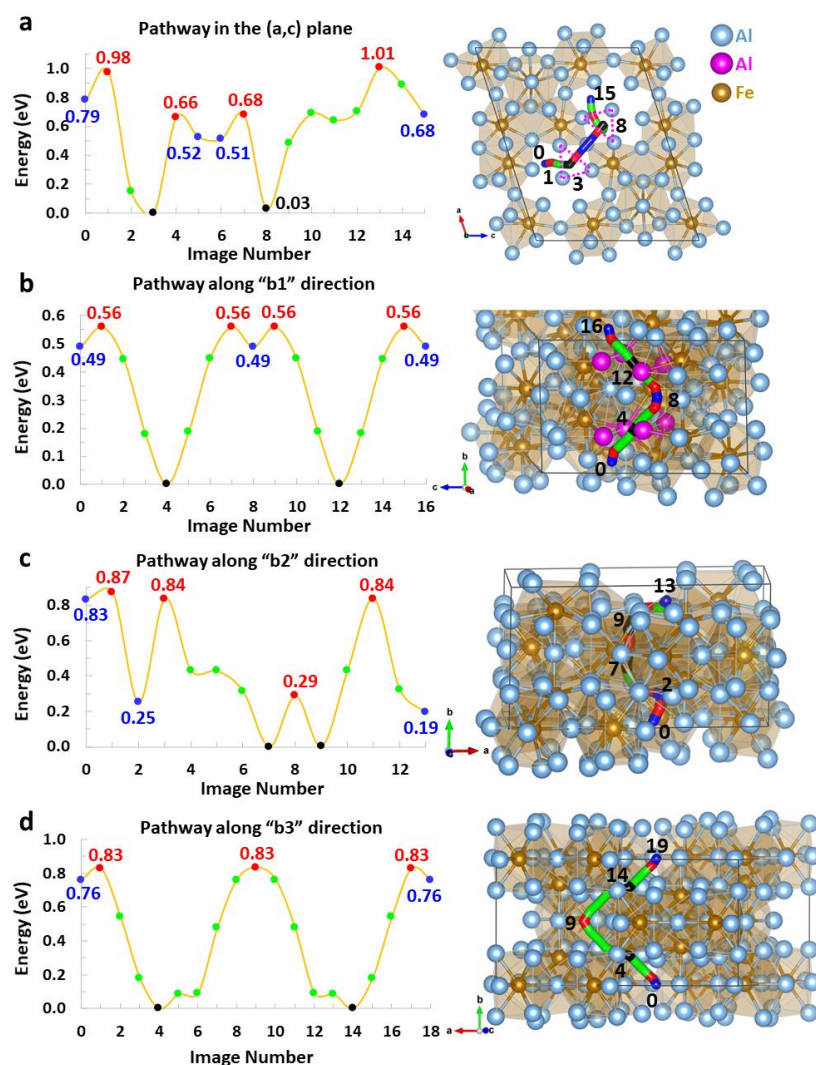


Figure 5: Energy diagrams and representation of the diffusion pathways for tritium in Fe₄Al₁₃. (a) Diffusion pathway in the (a,c) plane. (b-d) Three diffusion pathways across layers, along the *b*-

axis, labelled b1, b2, and b3. In the visual representations, some atoms have been removed for clarity. See main text for color-coding.

3.3 Tritium diffusion in Fe₂Al_x

Structures of the Fe₂Al_x phases. The various structures for the Fe₂Al_x phases have been generated from the orthorhombic Fe₂Al₅ (space group *Cmcm*, #63) experimental structure as determined by Burkhardt *et al.*⁹ The particularity of the Fe₂Al_x structures is that they have channels along the *c*-axis, as shown in Figure 6. As those channels have a variable occupancy of Al atoms, it was found that the Fe₂Al₅ stoichiometry is an approximate composition⁹ and *ab initio* simulations suggested that the stability of this phase would benefit from a slight excess of Al to yield a Fe₂Al_{5.6} stoichiometry.^{7,8} In order to capture the effects of partial Al occupancy in the channels on tritium diffusion, we have created three phases with different stoichiometries,⁸ namely Fe₂Al₄, Fe₂Al₅, and Fe₂Al₆, which structures are shown in Figure 6a, 6b, and 6c respectively. With these three stoichiometries, the proportion of Al vacancy in the channels varies from 100% in Fe₂Al₄, to 50% in Fe₂Al₅, and 0% in Fe₂Al₆. The relaxed lattice parameters for each phase are shown in Table 2 and compared to the experimental values of Fe₂Al₅. As expected, the best agreement is obtained for the Fe₂Al₅ stoichiometry, however, the calculated length of the *a*-axis is 3% shorter than the experimental value, probably due to the partial Al occupancy of the channels giving an approximate Fe₂Al₅ composition.

Fe-Al phase	<i>a</i> (Å)	<i>b</i> (Å)	<i>c</i> (Å)
Fe ₂ Al ₄	5.788 (-24.40%)	7.828 (+22.02%)	4.083 (-3.20%)
Fe ₂ Al ₅	7.422 (-3.06%)	6.459 (+0.69%)	4.183 (-0.83%)
Fe ₂ Al ₆	7.473 (-2.39%)	6.217 (-3.10%)	4.818 (+14.21%)
Experiment ⁹ (Fe ₂ Al ₅)	7.656	6.415	4.218

Table 2: Calculated relaxed lattice parameters for three Fe₂Al_x phases compared to experimental values for Fe₂Al₅. The variation from experiment are shown in brackets.

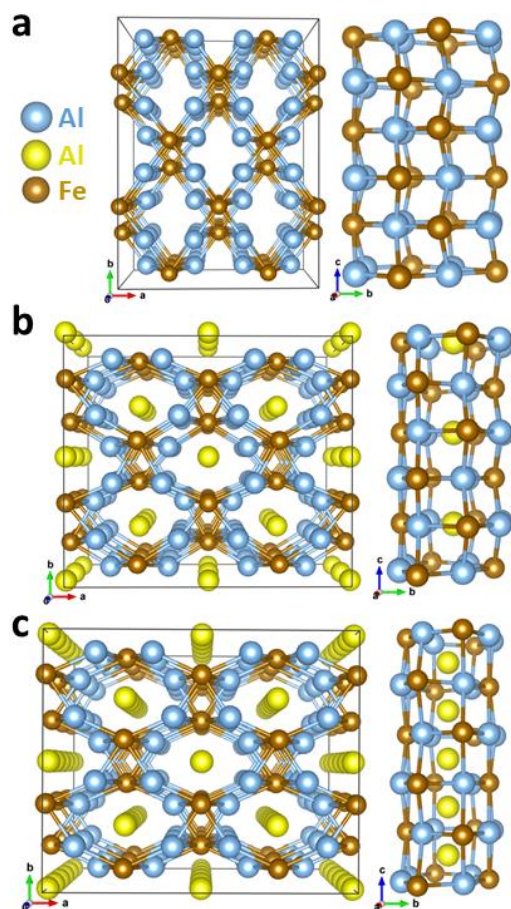


Figure 6: Representation of the bulk structure of orthorhombic Fe_2Al_x . Three stoichiometry have been investigated (a) Fe_2Al_4 (100% Al vacancy), (b) Fe_2Al_5 (50% Al vacancy), and (c) Fe_2Al_6 (0% Al vacancy). The Al atoms in the channels are represented by yellow balls.

Diffusion pathways in Fe_2Al_x . The diffusion pathway of tritium in each of the three structures has been investigated along the channels, following the direction of the c -axis. In the case of Fe_2Al_4 and 100% of Al vacancy, tritium diffuses at the center of the channel with a very small energy barrier of about 0.04 eV, as shown in Figure 7a. At the lowest energy positions, tritium forms two Al—T bonds of 1.871 Å with the Al of the channel's wall. For Fe_2Al_5 and 50% of Al vacancy, the diffusion of tritium is more complex as its position oscillates between the channel's center and the channel's wall, as shown in Figure 7b. The energy diagram shows that the lowest energy positions (images #6 to #8) are obtained when tritium is located at the center of the channel, in between two Al atoms labelled Al1 and Al2. In these positions the shortest Al—T distance is 1.553 Å (image #6), while the distance between Al1 and Al2 is 4.225 Å. Local minimum positions of tritium (images #0 and #16) have an energy of 0.66 eV and are obtained when tritium is at the channel's wall and forms Fe—T contacts of length 1.599 Å. Those local minimum positions periodically repeat every 4.190 Å in correlation with the Fe—Fe distance along the channel's wall. In contrast to a seemingly barrier-less diffusion in Fe_2Al_4 , the diffusion of tritium in Fe_2Al_5 involves a large energy barrier of 1.34 eV, suggesting that tritium is likely trapped at its lowest energy positions at the center of the channel, in between two Al atoms.

In the case of Fe_2Al_6 and 0% of Al vacancy, the diffusion of tritium is essentially occurring along the channel's wall, as shown in Figure 7c. Along this pathway, tritium hops between neighboring

Fe atoms along the channel's wall, separated by a distance of 3.198 Å. At the lowest energy positions, tritium forms a Fe—T bond of 1.566 Å and the energy barrier to overcome along this pathway is 0.18 eV.

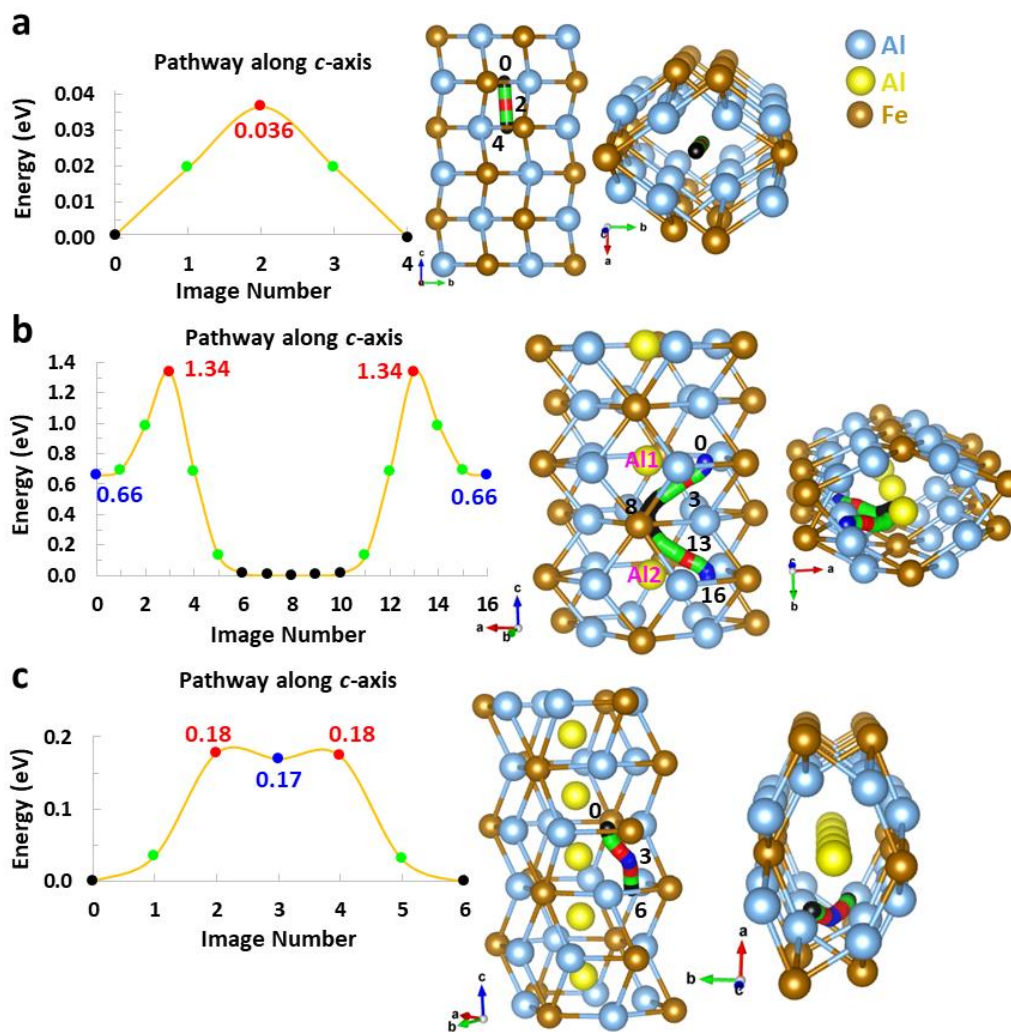


Figure 7: Energy diagrams and representation of the diffusion pathways for tritium in Fe_2Al_x phase. The diffusion pathway along the c -axis in (a) Fe_2Al_4 (100% Al vacancy), (b) Fe_2Al_5 (50% Al vacancy), and (c) Fe_2Al_6 (0% Al vacancy). The Al atoms in the channels are represented by yellow balls. In the visual representations, some atoms have been removed for clarity. See main text for color-coding.

3.4 Diffusion Coefficients

The diffusion coefficients of interstitial tritium, D_{T} , have been calculated by using the Einstein-Smoluchowski relation.¹⁷ The diffusion coefficients can be written as:

$$D_{\text{T}} = \frac{d^2}{c\tau} \quad (1)$$

where d and τ are the average distance and time between two jumps, respectively, and c is a parameter equal to 2 for one-dimensional, 4 for two-dimensional, and 6 for three-dimensional

diffusion. As DFT simulations are carried out at a temperature of 0 K, in the following we will neglect the entropy of migration in the equations and approximate the Gibbs free energy of migration by the migration enthalpy, E_a . While the vibrational motions induced by elevated temperatures could induce a slight change in the diffusion coefficients calculated in this work, we note that the energy barrier is almost unaffected by temperature changes.¹⁸

It should be noted that equation (1) does not consider the correlation effects between interstitial atoms. This is valid in our case since we are in a dilute interstitial solid solution, where every interstitial site around the interstitial solute is empty. Therefore, the diffusion coefficient can be written as:

$$D_T \approx \frac{d^2}{c} \nu_0 z e^{-\frac{E_a}{k_B T}} \quad (2)$$

where z is the coordination number and ν_0 is the attempt frequency which is typically of the order of the Debye frequency, ranging from 10^{12} to 10^{13} s^{-1} for practically all solids.¹⁷ Using statistical thermodynamics, Vineyard *et al.*¹⁹ has shown that the jump rate, ω , which is the number of jumps per second, has an Arrhenius-type dependence on temperature and can be written as:

$$\omega = \nu_0 e^{-\frac{E_a}{k_B T}} \quad (3)$$

The calculated diffusion coefficients and associated jump rates of interstitial tritium at two temperatures, 300 K and 600 K are summarized in Table 3. At 600 K, the calculated diffusion coefficients in FeNiAl₅ show that a diffusion along the *a*-axis is 1.04×10^{-13} $m^2 \cdot s^{-1}$, which is five orders of magnitude faster than along the *c*-axis. In Fe₄Al₁₃, the diffusion pathways along the *b*-axis are found to be from two to four orders of magnitude faster than in the (*a*,*c*) plane. The fastest diffusion pathway is obtained for the b1 pathway for which the diffusion coefficient is 2.07×10^{-12} $m^2 \cdot s^{-1}$ at 600 K. In the series of Fe₂Al_{*x*} phases, the diffusion coefficients at 600 K are 2.14×10^{-7} $m^2 \cdot s^{-1}$, 2.70×10^{-18} $m^2 \cdot s^{-1}$, and 1.27×10^{-8} $m^2 \cdot s^{-1}$ for Fe₂Al₄, Fe₂Al₅, and Fe₂Al₆ respectively. In this series, the diffusion coefficient for Fe₂Al₅ is lower by more than ten orders of magnitude compared to those of Fe₂Al₄ and Fe₂Al₆. This could be an artifact of the simulations in which the calculations of energy barriers using the NEB method requires to have static Al atoms in the channels, while in reality, those channels are fast diffusion pathways for Al.^{7,8} As shown in Figure 7b, the lowest energy positions for tritium in Fe₂Al₅ are at the center of the channel, in between two Al atoms. This suggests that tritium and Al diffusion in the channels are correlated. *Ab initio* simulations of Al diffusion along the channels of Fe₂Al₅ have been performed by Sakidja *et al.*⁸ and two pathways have been identified: (i) a straight line pathway, with a jumping distance of 2.37 Å and an energy barrier of 0.70 eV, and (ii) a curved pathway, with a jumping distance of 2.14 Å and an energy barrier of 0.52 eV. By using this information, and an average coordination number of 7, we calculated the diffusion coefficients for Al in the channels to be 2.59×10^{-12} $m^2 \cdot s^{-1}$ and 6.87×10^{-11} $m^2 \cdot s^{-1}$ at 600 K for the straight line and curved pathways respectively. Therefore, the lower limit of tritium diffusion in the channels of Fe₂Al₅ should be about 10^{-11} $m^2 \cdot s^{-1}$.

Altogether, we find that the diffusion of interstitial tritium at 600 K is faster in Fe₂Al_{*x*} phases, with $D_T \leq 10^{-11}$ $m^2 \cdot s^{-1}$, then in Fe₄Al₁₃ with $D_T \approx 10^{-12}$ $m^2 \cdot s^{-1}$, and finally in FeNiAl₅ with $D_T \approx 10^{-13}$ $m^2 \cdot s^{-1}$. Interestingly, all the diffusion coefficients calculated for Fe-Al phases are faster than that calculated for interstitial tritium in γ -LiAlO₂ which was in the order of $D_T \approx 10^{-14}$ $m^2 \cdot s^{-1}$.²⁰

Fe-Al phases	Diffusion Pathway	d (Å)	c	z	E_a (eV)	$T=300$ K		$T=600$ K	
						D_T ($m^2 \cdot s^{-1}$)	ω (jump/s)	D_T ($m^2 \cdot s^{-1}$)	ω (jump/s)
FeNiAl ₅	<i>a</i> -axis	4.50	6	1	0.78	3.22×10^{-20}	1	1.04×10^{-13}	3,092,335
	<i>c</i> -axis	1.33	6	1	1.19	2.90×10^{-28}	0	2.93×10^{-18}	991
Fe ₄ Al ₁₃	(<i>a,c</i>) plane	2.30	6	1	0.98	3.55×10^{-24}	0	5.60×10^{-16}	63,381
	<i>b</i> -axis (<i>b</i> 1)	2.50	6	1	0.56	4.09×10^{-17}	3,912	2.07×10^{-12}	$>1.98 \times 10^8$
	<i>b</i> -axis (<i>b</i> 2)	3.09	6	1	0.84	1.44×10^{-21}	0	1.51×10^{-14}	950,406
	<i>b</i> -axis (<i>b</i> 3)	2.58	6	1	0.83	1.42×10^{-21}	0	1.26×10^{-14}	$>1.13 \times 10^6$
Fe ₂ Al ₄	<i>c</i> -axis	2.07	2	2	0.04	1.07×10^{-7}	$>2.48 \times 10^{12}$	2.14×10^{-7}	$>4.98 \times 10^{12}$
Fe ₂ Al ₅	<i>c</i> -axis	3.00	2	1	1.34	1.62×10^{-29}	0	2.70×10^{-18}	60
Fe ₂ Al ₆	<i>c</i> -axis	2.82	2	1	0.18	4.06×10^{-10}	$>1.02 \times 10^{10}$	1.27×10^{-8}	$>3.20 \times 10^{11}$

Table 3: Calculated diffusion coefficients for interstitial tritium in several Fe-Al phases. The calculations used the following parameter values: $k_B=8.6173 \times 10^{-5}$ eV.K⁻¹ and $\nu_0=10^{13}$ s⁻¹.

Conclusion

The theoretical investigations of interstitial tritium diffusion pathways in various Al-rich (>60% at. Al) iron aluminide coating phases found that in FeNiAl₅ tritium prefers to diffuse in between layers, while in Fe₄Al₁₃, tritium prefers to diffuse across layers. In the case of Fe₂Al_x phases, the simulations show that the variable Al content in the channels affects the diffusion behavior of tritium in the channels. For 100% of vacancy, tritium prefers to diffuse at the center of the channel, while for 0% Al vacancy, tritium prefers to diffuse along the channel's wall. In the case where 50% Al vacancy are present in the channels, tritium can diffuse in a mixed way, with positions oscillating between the channel's center and wall. However, the large energy barrier involved in this case suggests that tritium diffusion could be correlated with Al diffusion in the channels.

While we found that at 600 K interstitial tritium diffuses faster in Fe₂Al_x phases ($D_T \leq 10^{-11} \text{ m}^2 \cdot \text{s}^{-1}$), then in Fe₄Al₁₃ ($D_T \approx 10^{-12} \text{ m}^2 \cdot \text{s}^{-1}$), and finally in FeNiAl₅ ($D_T \approx 10^{-13} \text{ m}^2 \cdot \text{s}^{-1}$), we also find that interstitial tritium generally diffuses faster in Fe-Al coating phases than in γ -LiAlO₂ pellet ($D_T \approx 10^{-14} \text{ m}^2 \cdot \text{s}^{-1}$).

Acknowledgments

This research was supported by the National Nuclear Security Administration (NNSA) of the U.S. Department of Energy (DOE) through the Tritium Science Research Supporting the Tritium Modernization Program (TMP) managed by Pacific Northwest National Laboratory (PNNL). The authors thank the PNNL Institutional Computing (PIC) facility for providing computational resources.

This report was prepared as an account of work sponsored by an agency of the United States Government. Neither the United States Government nor any agency thereof, nor any of their employees, makes any warranty, express or implied, or assumes any legal liability or responsibility for the accuracy, completeness, or usefulness of any information, apparatus, product, or process disclosed, or represents that its use would not infringe privately owned rights. Reference herein to any specific commercial product, process, or service by trade name, trademark, manufacturer, or otherwise does not necessarily constitute or imply its endorsement, recommendation, or favoring by the United States Government or any agency thereof. The views and opinions of authors expressed herein do not necessarily state or reflect those of the United States Government or any agency hereof.

4.0 References

1. Bums, K.A.; Love, E.F.; Thomhill, C.K. Description of the tritium-producing burnable absorber for the commercial light water reactor. *PNNL-22086 Rev. 19*, TTQP-1-015, Pacific Northwest National Laboratory (February 2012).
2. Senor, D.J. Science and technology in support of the tritium modernization program. Report PNNL-31479, Pacific Northwest National Laboratory (June 2021).
3. United States Government Accountability Office (GAO). National Nuclear Security Administration Needs to Ensure Continued Availability of Tritium for the Weapons Stockpile. *Report GAO-11-100 Nuclear Weapons* (October 2010).
4. Edwards, D.J.; Olszta, M.J.; Sunderland, D.J.; Devaraj, A.; Schemer-Kohrn, A.L.; Matthews, B.E. PIE of cycle 13 316SS cladding using aberration corrected STEM. Presentation at *Tritium Science Technical Exchange*, Virtual, Washington. PNNL-SA-156394 (September 2020).
5. Palm, M. The Al-Cr-Fe system-phases and phase equilibria in the Al-rich corner. *J. Alloys Compd.* **252**, 192-200 (1997).
6. Zamanzade, M.; Barnoush, A.; Motz, C. A review on the properties of iron aluminide intermetallics. *Crystals* **6**, 10 (2016).
7. Mihalkovič, M.; Widom, M. Structure and stability of Al_2Fe and Al_5Fe_2 : First-principles total energy and phonon calculations. *Phys. Rev. B* **85**, 014113 (2012).
8. Sakidja, R.; Perepezko, J.H., Calhoun, P. Synthesis, Thermodynamic Stability and Diffusion Mechanism of Al_5Fe_2 -Based Coatings. *Oxid. Met.* **81**, 167-177 (2014).
9. Burkhardt, U.; Grin, Y.; Ellner, M. Structure refinement of the iron-aluminium phase with approximate composition Fe_2Al_5 . *Acta Cryst.* **B50**, 313-316 (1994).
10. Kresse, G.; Furthmüller, J. Efficient iterative schemes for ab initio total-energy calculations using a plane-wave basis set. *Phys. Rev. B* **54**, 11169-11186 (1996).
11. Perdew, J.P.; Burke, K.; Ernzerhof, M. Generalized Gradient Approximation Made Simple. *Phys. Rev. Lett.* **77**, 3865-3868 (1996).
12. Eliner, M.; Röhrer, T. Zur Struktur der ternären Phase FeNiAl_5 /On the Structure of the Ternary Phase FeNiAl_5 . *Int. J. Mater. Res.* **81**, 847-849 (1990).
13. Grin, J.; Burkhardt, U.; Ellner, M.; Peters, K. Refinement of the $\text{Fe}_4\text{Al}_{13}$ structure and its relationship to the quasihomological homeotypical structures. *Z. Kristallogr. Krist.* **209**, 479-487 (1994).
14. Monkhorst, H.J.; Pack, J.D. Special points for Brillouin-zone integrations. *Phys. Rev. B* **13**, 5188 (1976).
15. Sheppard, D.; Terrell, R.; Henkelman, G. Optimization methods for finding minimum energy paths. *J. Chem. Phys.* **128**, 134106 (2008).
16. Sheppard, D.; Xiao, P.; Chemelewski, W.; Johnson, D.D.; Henkelman, G. A generalized solid-state nudged elastic band method. *J. Chem. Phys.* **136**, 074103 (2012).
17. Mehrer, H. Diffusion in solids: Fundamentals, methods, materials, diffusion-controlled processes. *Springer Series in Solid State Science*. 155 (2007).

18. Mantina, M.; Wang, Y.; Arroyave, R.; Chen, L.Q.; Liu, Z.K.; Wolverton, C. First-principles calculations of self-diffusion coefficients. *Phys. Rev. Lett.* **100**, 215901 (2008).
19. Vineyard, G.H. Frequency factors and isotropy effects in solid state rate processes. *J. Phys. Chem. Solids* **3**, 121-127 (1957).
20. Paudel, H.P.; Lee, Y.-L.; Senor, D.J.; Duan, Y. Tritium diffusion pathways in γ -LiAlO₂ pellets used in TPBAR: A first-principles density functional theory investigation. *J. Phys. Chem. C* **122**, 9755-9765 (2018).

Pacific Northwest National Laboratory

902 Battelle Boulevard
P.O. Box 999
Richland, WA 99354
1-888-375-PNNL (7665)

www.pnnl.gov